Simple non-fluorescent polarity labeling of microtubules for molecular motor assays

Virupakshi Soppina, Arpan K. Rai, and Roop Mallik
Department of Biological Sciences, Tata Institute of Fundamental Research, Mumbai, India

BioTechniques 46:543-549 (June 2009) doi 10.2144/000113124
Keywords: microtubule polarity labeling; molecular motor in vitro assays; avidin biotin labeling; kinesin dynein in vitro; bidirectional motion; magnetic bead labeling; motor reconstitution assay

Supplementary material for this article is available at www.BioTechniques.com/article/113124.

Transport of intracellular organelles along the microtubule cytoskeleton occurs in a bidirectional manner due to opposing activity of microtubule-associated motor proteins of the kinesin and dynein families. Regulation of this opposing activity and the resultant motion is believed to generate a polarized distribution of many organelles within the cell. The bidirectional motion can be reconstituted on in vitro assembled microtubules using organelles extracted from cells. This provides an opportunity to understand the regulation of intracellular transport through quantitative analysis of the motion of organelles in a controlled environment. Such analysis requires the use of polarity-labeled microtubules to resolve the plus and minus components of bidirectional motion. However, existing methods of in vitro microtubule polarity labeling are unsuitable for high-resolution recording of motion. Here we present a simple and reliable method that uses avidin-coated magnetic beads to prepare microtubules labeled at the minus end. The microtubule polarity can be identified without any need for fluorescence excitation. We demonstrate video-rate high-resolution imaging of single cellular organelles moving along plus and minus directions on labeled microtubules. Quantitative analysis of this motion indicates that these organelles are likely to be driven by multiple dynein motors in vivo.

Introduction

Long-distance intracellular transport relies on the microtubule (MT) cytoskeleton and MT-associated molecular motor proteins of kinesin and dynein families. MTs are polymerized protein filaments of α and β tubulin with a fast-growing plus end extending toward the cell periphery, and a minus end juxtaposed to the cell nucleus in interphase cells (1). MT-associated motor proteins are mechanochemical enzymes that carry cellular organelles (e.g., mitochondria, endosomes, melanosomes) as cargo along MTs using energy derived from ATP hydrolysis (1–3). Motor proteins of the kinesin and dynein families usually move toward MT-plus and minus directions within the cell respectively. Such MT-based motion is often bidirectional because of the presence and simultaneous activity of both kinds of motors on an individual cargo (1,4,5). The motors are hypothesized to exist on individual cargos within an "intracellular transport complex" that also includes non-motor proteins such as dynactin (6). This complex is believed to regulate net motion of the cargo in a manner that is poorly understood, but a topic of intense debate (1,4,5,7,8). The regulation of motion is important to understand, because it is largely responsible for the distribution of a multitude of organelles to distinct cellular locations. Live imaging and quantitative analysis of organelle motion inside a cell presents considerable difficulty, and has been demonstrated only in a few systems (7,9,10). An attractive alternative is to reconstitute the bidirectional motion of cellular organelles in controlled in vitro assays. Such reconstitution assays have been demonstrated for squid organelles (11), herpes virus (12), endosomes (13,14), vesicles (15,16), melanosomes (17), and other MT-motor driven cargos (18). If these assays are combined with high-resolution motion analysis, there is an excellent opportunity to understand the role of specific motor and non-motor proteins in the regulation of bidirectional intracellular transport.

To date, it has only been possible to obtain high-resolution data of in vitro motor-driven motion from experiments using motor-coated plastic beads. Analysis of the motion of beads has revealed biophysical properties of single motors such as processivity, velocity, step size, and response to load (19–21). Since these experiments use a purified motor, motion along the MT is unidirectional and predetermined (toward plus or minus end). It is therefore not necessary to have prior knowledge of the polarity of an MT on which motion is being assayed. In contrast to this, an organelle extracted from the cell can move in a bidirectional manner on the MT due to activity of both plus- and minus-directed motors. To identify the plus and minus components of motion and interpret it in terms of the activity of kinesin and dynein motors respectively, a priori knowledge of MT polarity is required.

Presently, two methods exist for the in vitro labeling of MT polarity. The first method relies on nucleation and extension of MTs from axonemes/centrosomes (16), which is then identified as the minus end of an MT. The use of this method has been limited to a few groups because the isolation of functional axonemes/centrosomes is difficult. In addition, MTs assembled from centrosomes are found to be bundled and overlapping, making it difficult to ascertain direction

and follow the motion of organelles over a long distance on a single MT (22). A second method uses fluorescently labeled tubulin to make a brightly fluorescent MT seed (23). The seed is then preferentially extended toward the MT plus end by adding a mixture of fluorescent and non-fluorescent tubulin. This results in a dimly fluorescent MT with a bright minus-end segment, and has been the popular method for microtubule polarity labeling for almost two decades. Unfortunately, this method is not suitable for high-resolution biophysical characterization of motor motion because of the following reasons: *(i)* simultaneous observation of dimly fluorescent MTs and non-fluorescent organelles in the same field is difficult, *(ii)* MT fluorescence gets quenched over the period of the assay, *(iii)* a long exposure (usually using an expensive camera) is required to image the weakly fluorescent MTs (finer details of bidirectional motion such as rapid reversals are therefore lost due to undersampling), *(iv)* fluorescently labeled MTs are known to break up into fragments upon exposure to light (24), and *(v)* intercalation of a fluorescent molecule into the MT could have unknown effects on motor function on the MT.

All of the above problems can be precluded if the MT label is visible under differential interference contrast (DIC) illumination. DIC microscopy is widely used to observe in vitro motor-driven motion of beads and organelles on MTs (21,25). Movies can be recorded at video rate [30 frames per second (fps)], and finer features of motion such as rapid reversals of bidirectional motion can be resolved. An infrared laser beam can be conveniently introduced into the optical path to combine motion analysis with single-molecule force measurements (21). An added advantage of a non-fluorescent MT label is the easy identification of individual MTs using the label as a guide to the eye. Here we present a simple non-fluorescent method that labels the MT minus end efficiently and reliably with magnetic beads. The label, along with the unlabeled portion of an MT, can be clearly observed by DIC microscopy. Long MTs (usually >40 µm) can be arranged in precisely parallel orientation, with no MT-MT overlaps. We establish the reliability of this labeling by assaying the plus-directed motion of beads coated with conventional kinesin, and demonstrate precise high-resolution position tracking of the motion of kinesin- and dynein-driven vesicles extracted from Dictyostelium cells on these labeled MTs.

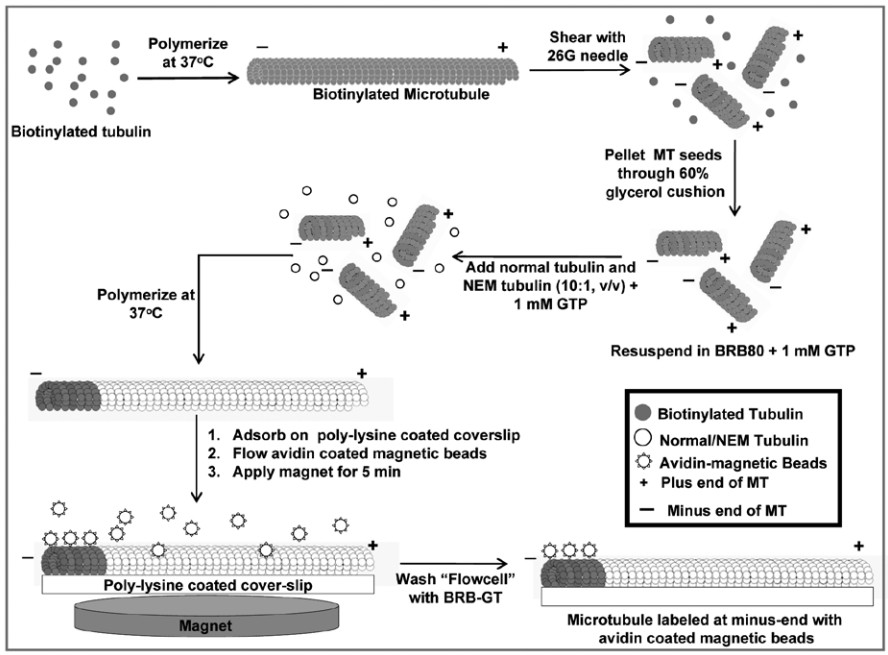

Figure 1. A schematic of the method for polarity labeling of microtubules using magnetic avidin-coated beads and biotinylated microtubule seeds. Details of the procedure can be found in the "Materials and methods" section.

Materials and methods

Unless otherwise mentioned, all chemicals were purchased from Sigma-Aldrich (Bengaluru, India).

Polarity labeling of microtubule minus ends with avidin-coated magnetic beads

The procedure is schematized in Figure 1. Biotinlyated tubulin was polymerized in the presence of 1 mM GTP and 20 µM taxol. Biotin-MTs prepared in this manner were sheared with 9 passages through a 26-guage needle to obtain short biotin-MT seeds. Biotin-MT seeds were pelleted by centrifugation [194000× *g*, 45 min, 37°C, 42.2 Ti rotor (Optima LE-80K; Beckman Coulter., Fullerton, CA, USA)] over BRB80 buffer (80 mM PIPES pH 6.8, 1 mM $MgCl_2$, 1 mM EGTA) containing 60% glycerol and 1 mM GTP. The pellet was resuspended in 15 µL BRB80 with 1 mM GTP. The biotin-MT seeds were preferentially extended from their plus ends with a mixture of normal and NEM-modified tubulin (in 10:1 molar ratio) in the presence of 1 mM GTP. MTs were stabilized by adding 100 µL of BRB-GT (BRB80 containing 1 mM GTP and 20 µM taxol). The resultant MTs were introduced into a flowcell prepared with a poly-L-lysine coated coverslip stuck to a glass slide with two thin strips of double-stick tape (21). The flowcell was washed with BRB-GT to remove unbound microtubules, and the

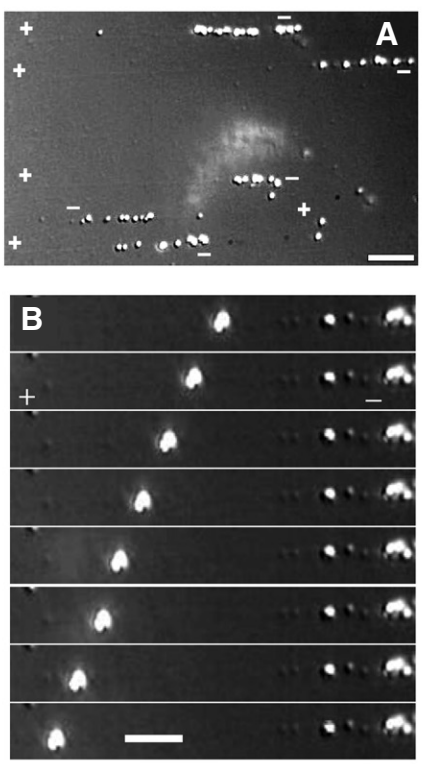

Figure 2. Representative image showing microtubules labeled at their minus ends with avidin-coated magnetic beads. Five low-contrast microtubules stretch horizontally across the field of view, and can be seen under careful observation. Plus and minus end of each microtubule is indicated. Scale bar = 5 µm. (B) Kinesin-1–driven motility of 500-nm latex bead. Frames are 2 s apart. Marker beads are visible at the right end. Scale bar = 3 µm. See Supplementary Movie 1.

coverslip surface was blocked with casein (5.5 mg/mL). Next, paramagnetic beads that were covalently conjugated to avidin (see "Avidin conjugation of magnetic beads" section for details) were introduced into the flowcell and a household magnet (diameter 2 cm, thickness 4 mm) was kept below the coverslip for 5 min to magnetically sediment the beads onto microtubules. The magnet was removed and unbound magnetic beads were washed out with BRB-GT. MT labeling was also verified (data not shown) with commercially available biotinylated tubulin (Cat. no. T333-A; Cytoskeleton, Denver, CO, USA) and avidin-conjugated magnetic beads (500-nm diameter; Ademtech, Pessac, France).

Avidin conjugation of magnetic beads

Carboxylated magnetic beads (340-nm diameter, Spherotech, Lake Forest, IL, USA) were incubated with 8 µM (w/v) Neutravidin (Pierce, Rockford, IL, USA) in 100 mM MES buffer (pH 6.7) for 15 min on a rotary shaker (Model no. T-345; Trishul Equipments, Mumbai, India). Freshly prepared 1-ethyl-3-(3-dimethyl-amino-propyl) carbodiimide (EDC; 73 µM final concentration) was added from 10 mg/mL stock and incubated for 1 h, after which the same amount of EDC was added again to the solution and incubated further for 1 h. The reaction was terminated by adding 1/5th volume of stop buffer (1% Triton X-100 in 10 mM Tris, pH 9.4). Beads were washed, re-suspended in phosphate buffer containing 0.03% fish skin gelatin (FSG) and stored at 4°C until further use.

Preparation and motility of Dictyostelium vesicles

Except for minor modifications, the procedure was identical to that reported earlier (16). Dictyostelium strain *Ax*-2 was grown in suspension at 22°C in HL-5 medium. Approximately 4–6 × 10^8 cells were collected by centrifugation. The cell pellet was washed once with ice-cold Sorenson's phosphate buffer (pH 6.0), centrifuged, and then resuspended in 1:1 w/v lysis buffer [30 mM Tris-HCl (pH 8.0), 4 mM EGTA, 3 mM DTT, 5 mM benzamidine HCl, 10 µg/mL soybean trypsin inhibitor, 5 µg/mL N-tosyl-L-phenylalanine chloromethyl ketone/N-tosyl-L-arginine methyl ester (TPCK/TAME), 10 µg/mL leupeptin, pepstatin A, chymostatin and 5 mM PMSF containing 30% (w/v) sucrose]. Cells were lysed by one passage through a 5-µm pore-size polycarbonate filter. The crude lysate was centrifuged (2000× *g*, 5 min, 4°C) to obtain a postnuclear supernatant (PNS).

Motion was observed using a motility mixture comprised of 18.5 µL lysis buffer/15% sucrose, 0.5 µL PNS and 1 µL of a 20× ATP regenerating mix (20 mM ATP, 20 mM $MgCl_2$, 40 mM creatine phosphate, and 40 U/mL creatine kinase). The motility mixture was introduced into a flowcell containing polarity-labeled MTs, as described earlier. Observation was done using a custom-modified DIC microscope (Nikon Instruments, Melville, NY, USA) using an oil immersion objective (Nikon 100×, 1.4 numerical aperture). All experiments were done at 25°C. In this manuscript we report the motion of spherical, refractile organelles which ranged 300–800 nm in size. A majority of these organelles are likely to be vesicles (including vacuoles), based on earlier published electron micrographs (26), and as also reported in earlier work on the motility of Dictyostelium extracts (15,16).

Preparation and motility of kinesin-1

Conventional kinesin (kinesin-1) was purified from fresh goat brain through a

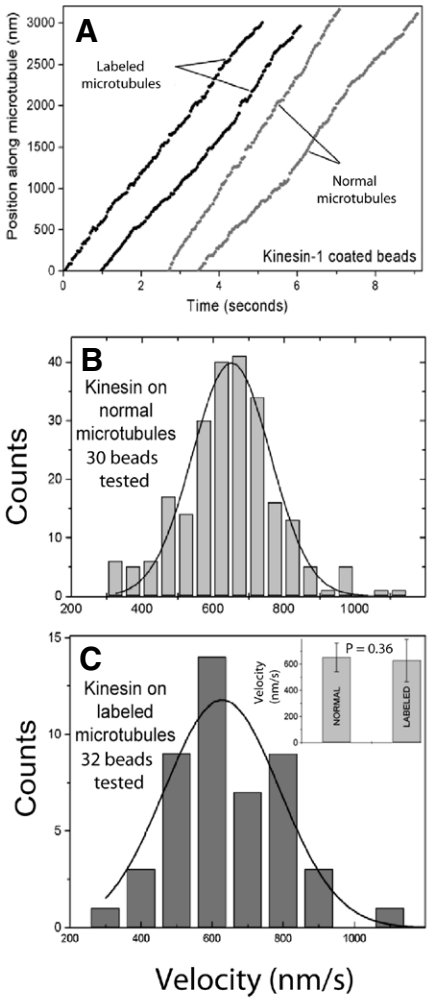

Figure 3. There is no difference between the motion of kinesin-1 on labeled and normal microtubules. (A) Typical video tracks of kinesin-1 coated beads moving on labeled and normal (unlabeled) microtubules. (B) Histogram of velocities for motion on normal microtubules. A Gaussian fit is superimposed. Velocity = 651.5 ± 110 nm/sec (mean ± SD). (C) Histogram of velocities for motion on labeled microtubules. Velocity = 627.7 ± 161.9 nm/sec (mean ± SD). Inset in (C) shows that the velocities are statistically same ($P = 0.36$, two-tailed Z-test).

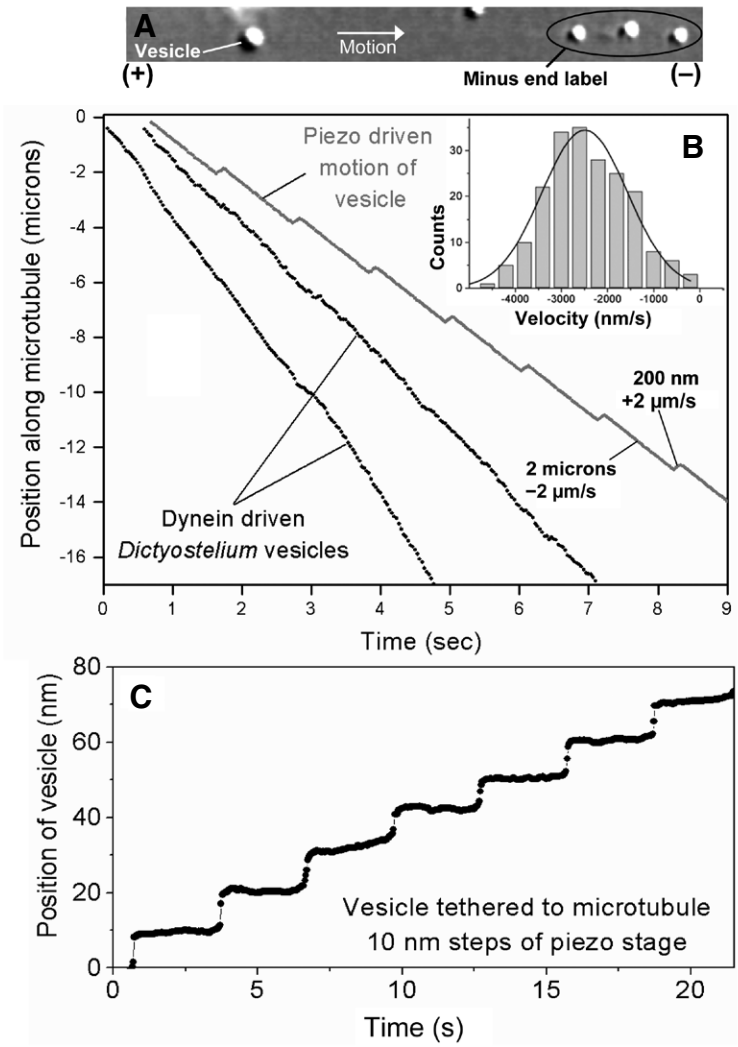

Figure 4. In vitro motion and particle tracking of extracted Dictyostelium vesicles. (A) Typical image of a vesicle on a labeled microtubule. Marker beads are visible at the right end. The low-contrast microtubule is not visible in this image, but may be seen in Supplementary Movie 2. (B) Representative video tracks of two minus-moving vesicles moving along polarity-labeled MTs. The motion is long and robust, with no backward (plus-directed) segments. The video track of a vesicle tethered to a labeled MT by motors, and moved with a piezoelectric device in alternating plus and minus directions is shown (velocities and distances are indicated in the figure). There is no motor-driven motion in this case because the experiment was done in absence of ATP. Backward (plus-directed) segments of motion are clearly resolved. Inset: Velocity distribution of dynein-driven vesicles obtained from parsing of video tracks into constant-velocity segments. A Gaussian fit is superimposed. The obtained velocity is 2.4 ± 0.9 µm/sec (mean ± SD). (C) A vesicle tethered to a labeled MT by motors in the absence of ATP is moved in steps of 10 nm using a piezoelectric stage. Individual steps are clearly resolved, establishing sub-pixel resolution in video tracking of Dictyostelium vesicles moving along labeled MTs.

nucleotide-dependent microtubule affinity procedure (27). No dynein or dynactin was detected in the purified sample as determined by SDS-PAGE and Western blotting with anti-dynein intermediate chain antibody (Santacruz, Santa Cruz, CA, USA) and anti-p150 glued antibody (BD Biosciences, San Jose, CA, USA). Kinesin-1 motility was assayed as described elsewhere (28). All experiments were done at 25°C.

Preparation of tubulin and modified tubulins

Tubulin was purified from fresh goat brain after two cycles of polymerization and depolymerization (29). Microtubule-associated proteins (MAPs) were removed through a final purification in high-molarity PIPES buffer (30). SDS-PAGE staining confirmed that the purity of this tubulin was comparable to commercially available purified tubulin (Cat. no. TL238-D; Cytoskeleton, Denver, CO, USA). No contamination from MAPs or tau was detected in a Western blot using an anti-MAP antibody. Biotinylation of tubulin was performed according to Hyman et al. (23) with some modifications. Microtubules were polymerized from tubulin (4.5 mg/mL) in BRB80 buffer (80 mM PIPES pH-6.8, 1 mM EGTA, and 1 mM $MgCl_2$) containing 1 mM GTP. To this, EZ Link Sulfo-NHS-LC-Biotin (Pierce, Rockford, IL, USA) was added to a final concentration of 2 mM. The mixture was incubated for 20 min at 37°C with occasional mixing. The reaction was terminated by adding potassium glutamate to a final concentration of 100 mM. Biotinylated microtubules were pelleted at 233,000× *g* for 1 h at 37°C over a pre-warmed cushion of BRB80 with 60% glycerol and 100 mM glutamate. The microtubule pellet was washed twice

with warm BRB80 before depolymerization with ice-cold BRB80 for 15 min. The biotin-tubulin was subjected to an additional cycle of polymerization and depolymerization to remove traces of free biotin. The supernatant containing biotinylated tubulin was centrifuged (194,000× *g*, 30 min, 4°C) to remove aggregates, and was then snap-frozen in liquid nitrogen. To prepare N-ethylmaleimide (NEM)–modified tubulin (23), purified tubulin (4.5 mg/mL) was thawed and incubated on ice for 10 min in the presence of 0.5 mM GTP and freshly prepared NEM (1 mM). Unreacted NEM was inactivated by incubation on ice for 10 min with β-mercaptoethanol (8 mM). Aliquots of the NEM-tubulin were snap-frozen in liquid nitrogen.

Microscopy and particle tracking

Polarity-labeled MTs, beads, and vesicles were observed under DIC illumination using the Nikon 100× oil immersion objective. Each pixel measured 98 nm × 98 nm at this magnification. Frames were acquired at video rate (30 fps, no binning) with a Cohu 4910 camera (Cohu, Poway, CA, USA). Image frames were digitized and saved as .AVI files using an image acquisition card (National Instruments, Bengaluru, India). No image processing hardware was used for image enhancement. The position of vesicles and beads was tracked frame by frame using custom written software (31) in Labview (National Instruments). The tracking algorithm calculates the position of the centroid of a cross-correlation image with sub-pixel resolution. The result of tracking is a 3-column text file containing time (T) and position coordinates (x,y) of the centroid of tracked object. Sub-pixel resolution was confirmed by moving a vesicle stuck on the coverslip in 10-nm steps using a piezo stage, and tracking its position (see Reference 31). The error in video tracking was determined to be ~3 nm from the standard deviation in position of a bead or vesicle stuck to the coverslip (31,32).

Parsing of video tracks into constant velocity segments

The video tracks were analyzed by a custom-written algorithm which determines the component of motion along a single microtubule, and then uses Bayesian optimization to parse the vesicle motion into segments of constant velocity (33). This algorithm has been extensively tested and validated earlier (20,32,33). Average velocity of vesicles and beads were obtained from a statistical analysis of velocity segments determined in the above manner.

Results

A simple method for preparationof non-fluorescent polarity-labeled microtubules

As outlined earlier, a non-fluorescent method of labeling the MT minus end would greatly improve quantitative high-resolution analysis of bidirectional motion on such MTs. To achieve this, we first prepared biotinylated microtubules and sheared them into short segments, which served as seeds for further nucleation of tubulin. The biotin-MT seeds were extended preferentially at the MT plus end using a mixture of normal (non-biotin) and NEM-modified tubulin (23). NEM is known to selectively inhibit microtubule polymerization at the MT minus end, possibly through a capping mechanism (34). Thus, long MTs with a short biotinylated minus-end segment were obtained. Such MTs were flowed in rapidly, into a flowcell with constant wicking at the other end using

Thousands of homogenizing applications at your fingertips.

Visit the Homogenizer Company at:
www.omni-inc.com/apps

OMNI International

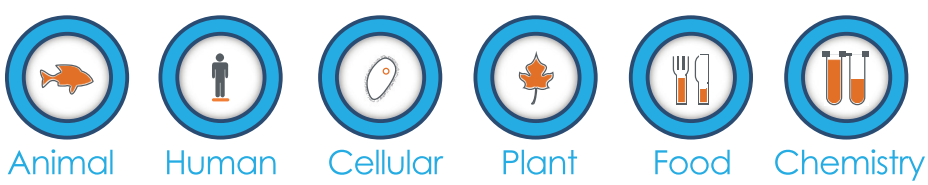

a filter paper (21). Numerous MTs adhered to the coverslip in an orientation parallel to the direction of flow because of shear force. While the MTs are physically in parallel orientation, the biotinylated MT minus ends have a random orientation. To identify the minus ends, avidin-coated magnetic beads were magnetically sedimented onto the MTs using a simple magnet kept beneath the coverslip. The minus-end biotin seed was then decorated with several magnetic beads that were clearly visible markers of MT polarity under DIC illumination (see Figure 2A). The use of a magnet greatly improves labeling efficiency; a comparative level of labeling could not be achieved without the magnet even after an incubation of 30 min. A schematic of the method is presented in Figure 1, and further details can be found in the Materials and Methods section. We scored an MT as labeled if three or more magnetic beads were attached to one end of the MT in close apposition (see Figure 2A). By this criterion, the MT labeling efficiency was found to be >60% (for example, 320 MTs labeled out of 500 in a flowcell). The parallel alignment of labeled MTs obtained by this method is ideal for motility assays with motors. Individual microtubules were ~50 μm in length, with a short (3–10 μm) magnetic bead–labeled biotin segment at the minus end (see Figure 2A). The length of labeled MTs was statistically the same as unlabeled MTs. We note that while this method of labeling is ideal for observing bead/organelle motion on MTs stuck to a coverslip, it might not be suitable for microtubule gliding assays on a motor-coated coverslip (35). This is because the avidin-coated marker beads can crosslink the biotinylated segments of MTs and therefore lead to clumping of MTs.

Reliable microtubule polarity labeling; labeled microtubules support robust motion of motors

To check the reliability of this MT-labeling method, we assayed kinesin-1 motion on the labeled MTs. An optical trap was used to place kinesin-1 coated polystyrene beads on labeled MTs (see "Materials and methods" section). The optical trap was switched off, and subsequent motion of the beads was recorded (see Figure 2B and Supplementary Movie 1). The reliability of polarity identification was >98%: out of 110 beads tested, 108 moved toward the MT plus end (away from the marker beads). The direction of motion could not be accurately determined for 2 beads due to apposing MTs. The kinesin-coated beads were earlier verified (data not shown) to move only toward the plus end of MTs using the conventional fluorescent MT-labeling method (23). Typical video tracks of kinesin-driven beads on normal (unlabeled) and labeled MTs are shown in Figure 3A. These tracks were parsed into segments of constant velocity (Figure 3, B and C) to obtain a histogram of the velocity distribution (see Reference 33; also see the "Materials and methods" section for details of velocity parsing). A statistical analysis of the velocities showed that MT labeling does not have any effect on kinesin motion (Figure 3C, inset). The position of individual beads on the labeled MTs could be tracked with a time resolution of 30 fps and a precision of ~3 nm. Such fast, high-resolution imaging is not possible with the fluorescent method of MT labeling.

Polarity-labeled microtubules support kinesin and dynein driven motion of vesicles extracted from Dictyostelium cells

As mentioned earlier, in vitro assays of bidirectional transport require polarity-labeled MTs. We now demonstrate the utility of this magnetic bead MT-labeling method in such assays using Dictyostelium as a model system (36). Bidirectional motion of vesicles extracted from Dictyostelium cells has been reconstituted on axoneme-labeled MTs earlier (15,16). Minus-directed vesicle motion in vitro is driven by cytoplasmic dynein (16) and plus-directed motion is mainly attributed (15) to a 245-kDa dimeric Unc104 kinesin (DdUnc104). We reconstituted this motion to observe (see Figure 4A) vigorous motion of vesicles toward both directions on labeled MTs (see the Materials and methods section for details of the reconstitution assay; Supplementary Movie 2 shows motion of dynein and kinesin driven vesicles on a single labeled MT). The position of single vesicles could be tracked with the same precision as beads (30 fps, ~3-nm accuracy). This is demonstrated in Figure 4C, where 10-nm piezo-driven steps of a single vesicle bound to an MT using dynein motor(s) is clearly resolved through video tracking. Since the direction of motion on a labeled MT is obvious, individual vesicles were identified to be driven by plus- or minus-directed motors. In our hands, approximately 20% of the moving vesicles were plus-directed (velocity 2.2 ± 0.8 μm/sec, mean ± SD), and 80% of moving vesicles were minus-directed (velocity 2.4 ± 0.9 μm/sec, mean ± SD; see Figure 4B, inset). These values are in close agreement with earlier in vitro (15,16) and in vivo (8,26) results. This establishes the reliability of this magnetic bead MT-labeling method in assaying bidirectional motion. We emphasize that in our magnetic bead MT-labeling method, motor-driven motion is observed on a segment of the MT which is normal (unlabeled). Any undesirable effect (24) of labeling groups on motor function or MT stability is therefore precluded. We could routinely observe fast and robust motion of Dictyostelium vesicles on the labeled MTs for >30 min.

Minus-directed vesicles move robustly over long distances

Representative video tracks of two minus-moving vesicles are presented in Figure 4B. More than 95% of minus-moving vesicles moved rapidly and robustly over a distance >15 μm. This motion would usually continue until the MT end was reached. Our earlier work with dynein-coated beads (32) has shown that such robust, long distance motion is driven by multiple (>3) dynein motors. To further investigate if vesicle motion is similar to beads driven by multiple dynein motors, we parsed the tracks into segments of constant velocity (see the "Materials and methods" section). A histogram of velocities for dynein-driven motion obtained in this manner is presented in Figure 4B, inset. We note that the distribution is a single Gaussian peak, with almost no instance of a pause (zero velocity) or backward motion (positive velocity). We confirmed that any backward (plus-directed) segments of vesicle motion >200 nm would have been detected easily in the video tracks. This was done by moving a vesicle bound to an MT in a back-and-forth manner using a piezo-electric device (see Figure 4C; short plus-directed segments are clearly resolved in the video track).

Discussion

We have presented a non-fluorescent method for minus-end labeling of MTs. In this method, the MT end-label along with the entire MT can be visualized under DIC illumination. The method is particularly suitable for in vitro reconstitution assays of motor-driven bidirectional motion with organelles extracted from cells. The plus and minus components of motion can be separated unambiguously and attributed to function of the corresponding motors. The high-resolution data obtained in this manner allows accurate statistical analysis of organelle motion on MTs. To demonstrate this point, we reconstituted and analyzed the motion of vesicles from Dictyostelium on the labeled MTs. Our preparation of labeled MTs with clearly defined polarity and length >40 μm provides a suitable platform to assay the vesicular motion, and resolve it into plus and minus-directed components with a precision and temporal resolution that has not been possible until now.

We focused on an aspect of dynein function inferred earlier from in vitro assays using dynein-coated beads (32,37). Beads driven by a single dynein motor or a single dynein-dynactin complex usually detach from the MT within 2 μm (6). High-

resolution analysis shows that this motion is erratic, with frequent pauses and backward (plus-directed) segments of motion up to 1 μm in length (32,37). However, increasing the number of dyneins brings about a qualitative change: the backward motion is suppressed, and the bead now moves robustly over long distances (>15 μm) on the MT (32). Thus, increasing dynein number can bring about qualitative changes in minus-end transport. Motion analysis of dynein-driven cellular organelles can therefore provide important clues about the putative number of dynein motors driving motion in vivo. This number is important to estimate, because it is an important parameter in hypothesizing models for the regulation of intracellular motor-driven transport (1,4,5,38,39). The statistical analysis of motion of minus-moving Dictyostelium vesicles on labeled MTs (Figure 4B) shows that these vesicles are likely to be transported by multiple dynein motors. It is likely that our experiments recapitulate the in vivo situation because the gentle and rapid preparation of vesicles employed here should introduce minimal perturbation of the vesicle membrane.

To conclude, we expect this new method of MT labeling to be used widely because the procedure is simple and uses reagents that are inexpensive and commercially available. Future studies will manipulate specific motors and motor-associated proteins on organelles to test current models of regulated intracellular transport (1,4,5).

Acknowledgments

R.M. acknowledges an International Senior Research Fellowship (grant no. WT079214MA) from the Wellcome Trust (UK). We thank S.J. King for help with kinesin purification and V. Nanjundiah for help with Dictyostelium culture. We also thank Avin Jayesh Ramaiya and Pradeep Barak for helpful discussions.

The authors declare no competing interests.

References

1. **Welte, M.A.** 2004. Bidirectional transport along microtubules. Curr. Biol. *14*:R525-R537.
2. **Mallik, R. and S.P. Gross.** 2004. Molecular motors: strategies to get along. Curr. Biol. *14*:R971-R982.
3. **Vale, R.D.** 2003. The molecular motor toolbox for intracellular transport. Cell *112*:467-480.
4. **Gross, S.P.** 2004. Hither and yon: a review of bi-directional microtubule-based transport. Phys. Biol. *1*:R1-R11.
5. **Muller, M.J., S. Klumpp, and R. Lipowsky.** 2008. Tug-of-war as a cooperative mechanism for bidirectional cargo transport by molecular motors. Proc. Natl. Acad. Sci. USA *105*:4609-4614.
6. **King, S.J. and T.A. Schroer.** 2000. Dynactin increases the processivity of the cytoplasmic dynein motor. Nat. Cell Biol. *2*:20-24.
7. **Kural, C., H. Kim, S. Syed, G. Goshima, V.I. Gelfand, and P.R. Selvin.** 2005. Kinesin and dynein move a peroxisome in vivo: a tug-of-war or coordinated movement? Science *308*:1469-1472.
8. **Ma, S. and R.L. Chisholm.** 2002. Cytoplasmic dynein-associated structures move bidirectionally in vivo. J. Cell Sci. *115*:1453-1460.
9. **Welte, M.A., S.P. Gross, M. Postner, S.M. Block, and E.F. Wieschaus.** 1998. Developmental regulation of vesicle transport in Drosophila embryos: forces and kinetics. Cell *92*:547-557.
10. **Nan, X., P.A. Sims, and X.S. Xie.** 2008. Organelle tracking in a living cell with microsecond time resolution and nanometer spatial precision. ChemPhysChem *9*:707-712.
11. **Vale, R.D., B.J. Schnapp, T.S. Reese, and M.P. Sheetz.** 1985. Organelle, bead, and microtubule translocations promoted by soluble factors from the squid giant axon. Cell *40*:559-569.
12. **Lee, G.E., J.W. Murray, A.W. Wolkoff, and D.W. Wilson.** 2006. Reconstitution of herpes simplex virus microtubule-dependent trafficking in vitro. J. Virol. *80*:4264-4275.
13. **Bananis, E., S. Nath, K. Gordon, P. Satir, R.J. Stockert, J.W. Murray, and A.W. Wolkoff.** 2004. Microtubule-dependent movement of late endocytic vesicles in vitro: requirements for dynein and kinesin. Mol. Biol. Cell *15*:3688-3697.
14. **Bananis, E., J.W. Murray, R.J. Stockert, P. Satir, and A.W. Wolkoff.** 2003. Regulation of early endocytic vesicle motility and fission in a reconstituted system. J. Cell Sci. *116*:2749-2761.
15. **Pollock, N., E.L. de Hostos, C.W. Turck, and R.D. Vale.** 1999. Reconstitution of membrane transport powered by a novel dimeric kinesin motor of the Unc104/KIF1A family purified from Dictyostelium. J. Cell Biol. *147*:493-506.
16. **Pollock, N., M.P. Koonce, E.L. de Hostos, and R.D. Vale.** 1998. In vitro microtubule-based organelle transport in wild-type Dictyostelium and cells overexpressing a truncated dynein heavy chain. Cell Motil. Cytoskeleton *40*:304-314.
17. **Rogers, S.L., I.S. Tint, P.C. Fanapour, and V.I. Gelfand.** 1997. Regulated bidirectional motility of melanophore pigment granules along microtubules in vitro. Proc. Natl. Acad. Sci. USA *94*:3720-3725.
18. **Cook, N.R. and H.W. Davidson.** 2001. In vitro assays of vesicular transport. Traffic *2*:19-25.
19. **Svoboda, K. and S.M. Block.** 1994. Force and velocity measured for single kinesin molecules. Cell *77*:773-784.
20. **Mallik, R., B.C. Carter, S.A. Lex, S.J. King, and S.P. Gross.** 2004. Cytoplasmic dynein functions as a gear in response to load. Nature *427*:649-652.
21. **Rice, S.E., T.J. Purcell, and J.A. Spudich.** 2003. Building and using optical traps to study properties of molecular motors. Methods Enzymol. *361*:112-133.
22. **Nielsen, E., F. Severin, J.M. Backer, A.A. Hyman, and M. Zerial.** 1999. Rab5 regulates motility of early endosomes on microtubules. Nat. Cell Biol. *1*:376-382.
23. **Hyman, A., D. Drechsel, D. Kellogg, S. Salser, K. Sawin, P. Steffen, L. Wordeman, and T. Mitchison.** 1991. Preparation of modified tubulins. Methods Enzymol. *196*:478-485.
24. **Vigers, G.P., M. Coue, and J.R. McIntosh.** 1988. Fluorescent microtubules break up under illumination. J. Cell Biol. *107*:1011-1024.
25. **Allen, R.D., N.S. Allen, and J.L. Travis.** 1981. Video-enhanced contrast, differential interference contrast (AVEC-DIC) microscopy: a new method capable of analyzing microtubule-related motility in the reticulopodial network of Allogromia laticollaris. Cell Motil. *1*:291-302.
26. **Roos, U.-P., M.D. Brabander, and R. Nuydens.** 1987. Movements of intracellular particles in undifferentiated amebae of *Dictyostelium discoideum*. Cell Motil. Cytoskeleton *7*:258-271.
27. **Schroer, T.A. and M.P. Sheetz.** 1991. Two activators of microtubule-based vesicle transport. J. Cell Biol. *115*:1309-1318.
28. **Vershinin, M., B.C. Carter, D.S. Razafsky, S.J. King, and S.P. Gross.** 2007. Multiple-motor based transport and its regulation by Tau. Proc. Natl. Acad. Sci. USA *104*:87-92.
29. **Sloboda, R.D. and J.L. Rosenbaum.** 1982. Purification and assay of microtubule-associated proteins (MAPs). Methods Enzymol. *85 Pt B*:409-416.
30. **Castoldi, M. and A.V. Popov.** 2003. Purification of brain tubulin through two cycles of polymerization-depolymerization in a high-molarity buffer. Protein Expr. Purif. *32*:83-88.
31. **Carter B.C., G.T. Shubeita, and S.P. Gross.** 2005. Tracking single particles: a user-friendly quantitative evaluation. Phys. Biol. *2*:60-72.
32. **Mallik R., D. Petrov, S.A. Lex, S.J. King, and S.P. Gross.** 2005. Building complexity: an in vitro study of cytoplasmic dynein with in vivo implications. Curr. Biol. *15*:2075-2085.
33. **Petrov, D.Y., R. Mallik, G.T. Shubeita, M. Vershinin, S.P. Gross, and C.C. Yu.** 2007. Studying molecular motor-based cargo transport: what is real and what is noise? Biophys. J. *92*:2953-2963.
34. **Phelps, K.K. and R.A. Walker.** 2000. NEM tubulin inhibits microtubule minus end assembly by a reversible capping mechanism. Biochemistry *39*:3877-3885.
35. **Howard, J., A.J. Hudspeth, and R.D. Vale.** 1989. Movement of microtubules by single kinesin molecules. Nature *342*:154-158.
36. **Koonce, M.P.** 2000. Dictyostelium, a model organism for microtubule-based transport. Protist *151*:17-25.
37. **Ross, J.L., K. Wallace, H. Shuman, Y.E. Goldman, and E.L. Holzbaur.** 2006. Processive bidirectional motion of dynein-dynactin complexes in vitro. Nat. Cell Biol. *8*:562-570.
38. **Kunwar, A., M. Vershinin, J. Xu, and S.P. Gross.** 2008. Stepping, strain gating, and an unexpected force-velocity curve for multiple-motor-based transport. Curr. Biol. *18*:1173-1183.
39. **Gross, S.P., M. Vershinin, and G.T. Shubeita.** 2007. Cargo transport: two motors are sometimes better than one. Curr. Biol. *17*:R478-R486.

Received 11 December 2008; accepted 5 February 2009.

Address correspondence to Roop Mallik, Department of Biological Sciences, Tata Institute of Fundamental Research, Homi Bhabha Road, Colaba, Mumbai, 400005, India. email: roop@tifr.res.in